Tracer diffusion of hard-sphere binary mixtures under nano-confinement

Umberto Marini Bettolo Marconi, Paolo Malgaretti, and Ignacio Pagonabarraga

Citation: The Journal of Chemical Physics **143**, 184501 (2015); doi: 10.1063/1.4934994
View online: http://dx.doi.org/10.1063/1.4934994
View Table of Contents: http://scitation.aip.org/content/aip/journal/jcp/143/18?ver=pdfcov
Published by the AIP Publishing

Tracer diffusion of hard-sphere binary mixtures under nano-confinement

Umberto Marini Bettolo Marconi,[1,a)] Paolo Malgaretti,[2,3,4,b)] and Ignacio Pagonabarraga[4,c)]
[1]*Scuola di Scienze e Tecnologie, Università di Camerino, Via Madonna delle Carceri, 62032 Camerino, Italy and INFN Perugia, Perugia, Italy*
[2]*Max-Planck-Institut für Intelligente Systeme, Heisenbergstr. 3, D-70569 Stuttgart, Germany*
[3]*IV. Institut für Theoretische Physik, Universität Stuttgart, Pfaffenwaldring 57, D-70569 Stuttgart, Germany*
[4]*Departament de Fisica Fonamental, Universitat de Barcelona, Av. Martí i Franques 1, Barcelona, Spain*

(Received 1 July 2015; accepted 20 October 2015; published online 10 November 2015)

The physics of diffusion phenomena in nano- and microchannels has attracted a lot of attention in recent years, due to its close connection with many technological, medical, and industrial applications. In the present paper, we employ a kinetic approach to investigate how the confinement in nanostructured geometries affects the diffusive properties of fluid mixtures and leads to the appearance of properties different from those of bulk systems. In particular, we derive an expression for the friction tensor in the case of a bulk fluid mixture confined to a narrow slit having undulated walls. The boundary roughness leads to a new mechanism for transverse diffusion and can even lead to an effective diffusion along the channel larger than the one corresponding to a planar channel of equivalent section. Finally, we discuss a reduction of the previous equation to a one dimensional effective diffusion equation in which an entropic term encapsulates the geometrical information on the channel shape. © *2015 AIP Publishing LLC*. [http://dx.doi.org/10.1063/1.4934994]

I. INTRODUCTION

The recent interest for the transport phenomena of gases or liquids confined in spaces whose span is comparable to the molecular size is motivated by the important technological, medical, and industrial applications of nanofluidics so diverse as DNA sequencing, element separation, or energy harvesting. It is well known that confinement can have a strong impact on both the static and dynamic properties of fluids.[1,2] The systematic theoretical study that confinement has on the behavior of fluids has concentrated on straight channels, hence overlooking the potential impact that the shape of the bounding walls may have on the collective properties of confined fluids. Recent studies have shown that the coupling between the system and the geometrical constraints overimposed by the environment can be relevant in situations such as molecular transport in zeolites,[3] ionic channels,[4] or in microfluidic devices.[5,6] Moreover, geometrical constraints can induce novel dynamical scenarios, such as particle separation,[7] cooperative rectification,[8,9] and negative mobility[10,11] that are absent in the behavior of the corresponding systems in bulk.

In the present paper, we will analyze the impact that the corrugation of the confining walls has in the diffusion of model non-ideal fluids. Specifically, we will concentrate on a hard sphere binary fluid mixture composed by two components, say A and B, with different sizes, and will consider the tracer limit of larger component, B. We shall show that to take into account the wall roughness, one has to modify the Fick equation for the concentration of B particles, $c(\mathbf{r},t)$,

$$\frac{\partial}{\partial t}c(\mathbf{r},t) = D_0\nabla^2 c(\mathbf{r},t), \tag{1}$$

where D_0 is the bulk diffusion coefficient.

Our treatment considers a binary hard sphere mixture between hard walls, perhaps the most basic model of confinement of non-ideal gases, which has the ability to capture the essential physics of inhomogeneous fluids, such as variations of the density near the walls, layering, and solid-fluid transition. We associate the majority component with the solvent and the minority component with the solute, whose concentration is negligible, the so called tracer limit and base the description of the diffusion process on the equations for the partial densities and the momentum density, which have been previously obtained using a Boltzmann-Enskog approach,[12] which accounts for the excluded volume effect, due to the finite size of the molecules. In the tracer limit, since the majority species is virtually unaffected by the motion of the dilute species, we are able to derive a simplified equation for the tracer concentration.

In the second part of the paper following a seminal idea of Jacobs,[13] we further reduce the complexity of the problem, by contracting the description from a three dimensional problem, to a one dimensional effective problem, which is mapped onto a diffusion process along the pore axis in the presence of a so called entropic potential. Such a reduction was introduced heuristically by Jacobs many years ago and revisited by Zwanzig, Kalinay-Percus, Reguera-Rubi, Dagdug-Bezrukov-Berezhkovskii, and coworkers among others who gave a statistical mechanical foundation to it.[14–23]

Finally, the magnitude of the coupling between the microscopic interactions of the medium and the mesoscopic modulation of the confinement is discussed.

a)umberto.marinibettolo@unicam.it
b)malgaretti@is.mpg.de
c)ipagonabarraga@ub.edu

II. THE KINETIC APPROACH

In a recent series of papers, one of the authors has developed a Boltzmann-Enskog self-consistent theory for fluid mixtures in inhomogeneous environment[12,24] and has provided a microscopic derivation of the equations governing the evolution of concentration fluctuations in an M-component mixture of hard-spheres of diameters $\sigma_{\alpha\alpha}$ and masses m^α, where $\alpha = 1, M$. The analysis of the kinetic equations for the individual species leads to the conservation law of the local number density of species, $n^\alpha(\mathbf{r},t)$,

$$\frac{\partial}{\partial t} n^\alpha(\mathbf{r},t) + \nabla \cdot \left(n^\alpha(\mathbf{r},t)\mathbf{u}^\alpha(\mathbf{r},t) \right) = 0 \tag{2}$$

and to the balance equation for the associated momentum density,

$$\frac{\partial}{\partial t}[n^\alpha(\mathbf{r},t)u_j^\alpha(\mathbf{r},t)] + \nabla_i \left(n^\alpha(\mathbf{r},t)u_i^\alpha(\mathbf{r},t)u_j^\alpha(\mathbf{r},t) - n^\alpha(\mathbf{r},t)w_i^\alpha(\mathbf{r},t)w_j^\alpha(\mathbf{r},t) \right)$$
$$= -\frac{1}{m^\alpha}\nabla_i \pi_{ij}^\alpha - \frac{\nabla_j V^\alpha(\mathbf{r})}{m^\alpha} n^\alpha(\mathbf{r},t) + \frac{n^\alpha(\mathbf{r},t)}{m^\alpha}\left(\mathbf{F}^{\alpha,mf}(\mathbf{r},t) + \mathbf{F}^{\alpha,drag}(\mathbf{r},t) + \mathbf{F}^{\alpha,viscous}(\mathbf{r},t) \right), \tag{3}$$

where $\mathbf{u}^\alpha$ is the average velocity of component α, $\mathbf{w}^\alpha = (\mathbf{u}^\alpha - \mathbf{u})$ is the relative average velocity of species α with respect to the center of mass velocity, $\mathbf{u}$, of the mixture.

The tensor $\pi_{ij}^\alpha(\mathbf{r},t)$, in analogy with pure fluids, represents the kinetic contribution to the partial stress tensor

$$\pi_{ij}^\alpha(\mathbf{r},t) = k_B T \delta_{ij} n^\alpha(\mathbf{r},t). \tag{4}$$

Eq. (3), besides the external body force $-\nabla_j V^\alpha$, contains three kinds of forces of different nature, resulting from the analysis of the microscopic Enskog collision operator:[25,26] a mean force, a drag force, and a viscous force. Specifically, $\mathbf{F}^{\alpha,mf}$ is the reversible force acting on α particles at $\mathbf{r}$ due to the influence of all remaining particles,

$$\mathbf{F}^{\alpha,mf}(\mathbf{r},t) = -k_B T \sum_\beta \sigma_{\alpha\beta}^2 \times \int d\hat{\mathbf{s}}\hat{\mathbf{s}} g_{\alpha\beta}(\mathbf{r}, \mathbf{r} + \sigma_{\alpha\beta}\hat{\mathbf{s}}, t) n_\beta(\mathbf{r} + \sigma_{\alpha\beta}\hat{\mathbf{s}}, t), \tag{5}$$

where $\hat{\mathbf{s}}$ is a unit vector of components $(\sin\theta\cos\phi, \sin\theta\sin\phi, \cos\theta)$, $\int d\hat{\mathbf{s}} \equiv \int_0^{2\pi} d\phi \int_0^\pi d\theta \sin\theta$ indicates integration over the unit sphere, $g_{\alpha\beta}$ is the inhomogeneous hard sphere pair correlation function at contact, and $\sigma_{\alpha\beta} = (\sigma_{\alpha\alpha} + \sigma_{\beta\beta})/2$. Such a force is the gradient of the so-called potential of mean force and can be identified with the gradient of the excess chemical potential of species α over the ideal gas value, $\mu_{int}^\alpha(\mathbf{r})$ according to

$$\mathbf{F}^{\alpha,mf}(\mathbf{r},t) = -\boldsymbol{\nabla}\mu_{int}^\alpha(\mathbf{r},t) \tag{6}$$

whereas the corresponding total chemical potential is given by $\mu^\alpha(\mathbf{r}) = k_B T \ln n^\alpha(\mathbf{r}) + \mu_{int}^\alpha(\mathbf{r})$. The drag force is purely dissipative, local and is proportional to the difference of velocities of unlike species,

$$F_i^{\alpha,drag}(\mathbf{r},t) = -\sum_\beta \boldsymbol{\gamma}_{ij}^{\alpha\beta}(\mathbf{r},t)(u_j^\alpha(\mathbf{r},t) - u_j^\beta(\mathbf{r},t)) \tag{7}$$

via the inhomogeneous friction tensor $\gamma_{ij}^{\alpha\beta}$ which is associated to the interactions and relative motion between the different species. Finally, the dissipative force $\mathbf{F}^{\alpha,viscous}$ represents the viscous force acting on species α due to velocity gradients and in the present treatment, it will be neglected under the assumption that the velocity varies slowly.[27]

The details of the procedure which allows to reduce the coupled differential equations for the densities and for the momenta of the species to a diffusion equation for the concentration are described in Refs. 12 and 24. The assumptions are (a) that since the typical fluid velocities in micro and nanofluidic systems are low, we can neglect the non-linear terms, (b) the velocity gradients are negligible so that we can discard viscous forces and retain only the diffusive terms, and (c) the acceleration of the species with respect to the center of mass is negligible.

For hard sphere mixtures, the friction tensor in the Enskog model can be computed explicitly and reads

$$\gamma_{ij}^{\alpha\beta}(\mathbf{r},t) = 2\sigma_{\alpha\beta}^2 \sqrt{\frac{2\mu_{\alpha\beta}k_B T}{\pi}} \times \int d\hat{\mathbf{s}} s_i s_j g_{\alpha\beta}(\mathbf{r}, \mathbf{r} + \sigma_{\alpha\beta}\hat{\mathbf{s}}, t) n^\beta(\mathbf{r} + \sigma_{\alpha\beta}\hat{\mathbf{s}}, t), \tag{8}$$

where $\mu_{\alpha\beta} = m^\alpha m^\beta/(m^\alpha + m^\beta)$ is the reduced mass.

For a binary mixture of hard-spheres, it is useful to define the local mass concentration $c(\mathbf{r},t) = \frac{\rho^B(\mathbf{r},t)}{\rho(\mathbf{r},t)}$, with $\rho^B = m^B n^B$ and $\rho = m^A n^a + m^B n^B$. Using the results of Ref. 24, when the fluid velocity is negligible and in the absence of external forces, the balance equation for the local mass concentration reduces to

$$\frac{\partial}{\partial t} c(\mathbf{r},t) = \frac{1}{\rho(\mathbf{r},t)} \nabla_i \cdot \left(\rho(\mathbf{r},t)c(\mathbf{r},t)(1 - c(\mathbf{r},t))(\gamma_{ij}^{-1}(\mathbf{r},t)) \times \nabla_j \left(\frac{\mu^B(\mathbf{r},t)}{m^B} - \frac{\mu^A(\mathbf{r},t)}{m^A} \right) \right), \tag{9}$$

where we have introduced the symmetrized inhomogeneous friction tensor, $\gamma_{ij} = \frac{\gamma_{ij}^{AB}}{m^A} + \frac{\gamma_{ij}^{BA}}{m^B}$ and its inverse γ_{ij}^{-1}. Neglecting the variations in the density around a reference sphere, the friction tensor reduces to $\gamma_{ij} = \gamma\delta_{ij}$. We can then derive an approximate, explicit expression for γ from Eq. (8),

$$\gamma = \frac{8}{3}\rho \frac{\sqrt{2\pi\mu_{AB}k_B T}}{m^A m^B} g_{AB}\sigma_{AB}^2 \tag{10}$$

and rewrite the conservation equation for the local mass concentration as a standard diffusion equation

$$\frac{\partial}{\partial t} c(\mathbf{r},t) = D^{AB}\nabla^2 c(\mathbf{r},t), \tag{11}$$

in terms of the mutual diffusion coefficient, D^{AB},

$$D^{AB} = \frac{k_B T}{\gamma} \frac{\rho}{n} \frac{1}{m^A m^B}, \tag{12}$$

which relates the friction and the diffusion coefficients through the Einstein fluctuation-dissipation relation.

III. DIFFUSION IN CONFINED STRUCTURES

The general framework described in Sec. II also holds for a nanoconfined mixture. To analyze its dynamic features, we consider the specific case where the fluid is confined to a symmetric slit bound by two non-intersecting walls identified, in the Monge representation, by the two height functions $z = \pm h(x)$. Accordingly, the fluid densities will be symmetric with respect to the midplane $z = 0$ and translationally invariant along the y direction. Each species, α, composing the fluid mixture is confined to the slit due to the wall potential they will experience,

$$V^{\alpha}(\mathbf{r}) = \begin{cases} V^{\alpha}_{soft}(\mathbf{r}) & z < |h(x)| \\ \infty & else \end{cases} \tag{13}$$

that is the sum of a soft attractive potential, V^{α}_{soft}, of general functional form and of a harshly repulsive confining potential. The densities of the fluid species are no longer homogeneous due to the presence of the confining solid walls. As a result, the friction matrix, Eq. (8), is no longer diagonal. The inhomogeneous nature of the pair correlation function at contact, g_{AB}, encodes the response of the mixture to such inhomogeneities. Although an exact functional form of the pair distribution function under generic inhomogeneous conditions is not known, we resort to a two-component generalization[28] of the Fisher-Methfessel prescription,[29] which states that the functional form of the inhomogeneous $g_{AB}(\mathbf{r}, \mathbf{r} + \sigma_{AB}\hat{\mathbf{s}})$ can be obtained from the Carnahan-Starling expression for the bulk pair correlation of mixtures at pair contact, g^{bulk}_{AB},[30,31]

$$g^{bulk}_{AB}(\{\xi_n\}) = \frac{1}{1-\xi_3} + \frac{3}{2}\frac{\sigma_{AA}\sigma_{BB}}{\sigma_{AB}}\frac{\xi_2}{(1-\xi_3)^2} + \frac{1}{2}\left(\frac{\sigma_{AA}\sigma_{BB}}{\sigma_{AB}}\right)^2 \frac{\xi_2^2}{(1-\xi_3)^3}, \tag{14}$$

where the ξ_n are linear combinations of the bulk densities $\xi_n = \frac{\pi}{6}\sum_{\alpha} n^{\alpha}\sigma^n_{\alpha\alpha}$. In an inhomogeneous environment, g_{AB} is generalized replacing the bulk densities n^A and n^B by the corresponding inhomogeneous coarse grained densities $\bar{n}^A(\mathbf{r})$ and $\bar{n}^B(\mathbf{r})$. These are the averages over spheres of volume $\omega_{\alpha} = \pi\sigma^3_{\alpha\alpha}/6$ centered at $\mathbf{r}$,

$$\bar{n}^{\alpha}(\mathbf{r}) = \frac{1}{\omega_{\alpha}} \int d\mathbf{r}' n^{\alpha}(\mathbf{r}+\mathbf{r}')\, \theta\left(\frac{\sigma_{\alpha\alpha}}{2} - |\mathbf{r}-\mathbf{r}'|\right).$$

Accordingly, we assume that the spatial dependence of the pair correlation function at contact enters through its dependence on the inhomogeneous coarse grained densities. Hence, from Eq. (14), we arrive at

$$g_{AB}(\mathbf{r}, \mathbf{r} + \sigma_{AB}\hat{\mathbf{s}}) = g^{bulk}_{AB}(\{\bar{\xi}_n(\mathbf{r} + \frac{1}{2}\hat{\mathbf{s}}\sigma_{AB})\}), \tag{15}$$

where the smeared functions $\bar{\xi}_n$ are

$$\bar{\xi}_n(\mathbf{r}) = \frac{\pi}{6}\bar{n}^A(\mathbf{r})\sigma^3_{AA} + \frac{\pi}{6}\bar{n}^B(\mathbf{r})\sigma^3_{BB}.$$

Substituting Eq. (15) into Eq. (8), we get

$$\begin{pmatrix} \gamma_{XX}(x,z) \\ \gamma_{ZZ}(x,z) \\ \gamma_{XZ}(x,z) \end{pmatrix} = \frac{2\sigma^2_{AB}}{m^B}\sqrt{\frac{2\mu_{AB}k_BT}{\pi}} \times \int d\hat{\mathbf{s}} \left\{ \begin{pmatrix} s_X s_X \\ s_Z s_Z \\ s_X s_Z \end{pmatrix} g^{bulk}_{AB}(\{\bar{\xi}_n(\mathbf{r} + \frac{\hat{\mathbf{s}}\sigma_{AB}}{2})\}) \times \left[\frac{n^A(\mathbf{r}+\hat{\mathbf{s}}\sigma_{AB})}{m^A} + \frac{n^B(\mathbf{r}+\hat{\mathbf{s}}\sigma_{AB})}{m^B}\right]\right\} \tag{16}$$

which shows that the geometric confinement leads, generically, to a tensorial friction coefficient that deviates from its bulk behavior. As we will analyze subsequently, the geometrically induced off-diagonal components imply that in general, under confinement, non-ideal fluid mixtures will show transverse diffusion These off-diagonal components vanish for planar interfaces, hence showing that transverse diffusion develops only as a combination of particle interaction and spatially varying confinement. Specifically, if we consider flat walls, Eq. (16) reduces to

$$\begin{pmatrix} \gamma_{XX}(x,z) \\ \gamma_{ZZ}(x,z) \end{pmatrix} = \frac{2\sigma^2_{AB}}{m^B}\sqrt{2\pi\mu_{AB}k_BT} \times \int_{-1}^{1} d\hat{s}_Z \left\{ \begin{pmatrix} 1-\hat{s}^2_Z \\ 2\hat{s}^2_Z \end{pmatrix} g^{bulk}_{AB}(\{\bar{\xi}_n(z+\frac{1}{2}\sigma_{AB}\hat{s}_Z)\}) \times \left[\frac{n^A(z+\sigma_{AB}\hat{s}_Z)}{m^B} + \frac{n^B(z+\sigma_{AB}\hat{s}_Z)}{m^A}\right]\right\}. \tag{17}$$

These expressions are equivalent to those obtained by Davis and coworkers for slit-like pores by using a method based on the Born-Green-Yvon equation.[32–35]

IV. DIFFUSION EQUATION FOR n^B IN THE TRACER LIMIT

The results obtained in Sec. III hold for a general binary mixture of hard spheres. When one of the components of the binary mixture becomes extremely diluted ($n^B << n^A$), the method described in Secs. I–III to derive the corresponding diffusion equations for the mixture dynamics considerably simplifies and one can arrive at more explicit expressions for the diffusive fluxes. In the tracer limit, in fact, we may disregard the B-B interactions and the friction matrix governing the diffusion of B particles turns out to be independent from the density profile of the B-particles and is solely a functional of the solvent density profile, $n^A(\mathbf{r}, t)$. In the following, we treat the case of a system prepared in a state where the majority component A, identified with the solvent, is at thermodynamic equilibrium, so that $\mathbf{u} = 0$ and its density satisfies the balance condition:

$$\nabla(\mu^A(\mathbf{r}) + V^A(\mathbf{r})) = 0. \tag{18}$$

Although it will not be pursued in the rest of this contribution, the method we will introduce can be easily generalized to non-equilibrium situations where the dynamics of A particle is known and independent of the B particles.

If we specialize general Eq. (1) for the tracer species, with density n^B, and use Eq. (2) to relate the velocity of the tracer species to local forces, we arrive at

$$\frac{\partial}{\partial t}n^B(\mathbf{r},t) = \nabla_i \cdot \left(n^B(\mathbf{r},t)\gamma_{ij}^{-1}(\mathbf{r},t)\Big[\frac{1}{m^B}\nabla_j(\mu^B(\mathbf{r}) + V^B(\mathbf{r})) - \frac{1}{m^A}\nabla_j(\mu^A(\mathbf{r}) + V^A(\mathbf{r}))\Big]\right), \tag{19}$$

where in this limit, γ_{ij}^{-1} reduces to the ij matrix element of the matrix inverse of $\gamma_{ij} = \frac{1}{m^B}\gamma_{ij}^{BA}$.

For the confining slit, Eq. (13), which is translational invariant along the y-direction, the relevant components of the flux of the tracer species in response to density gradients or externally applied forces read

$$J_X^B(x,z) = -\frac{n^B(x,z,t)}{m_B}\left(\gamma_{XX}^{-1}(x,z)(\nabla_X\mu^B(x,z,t) + \nabla_X V^B(\mathbf{r})) + \gamma_{XZ}^{-1}(x,z)(\nabla_Z\mu^B(x,z,t) + \nabla_Z V^B(\mathbf{r}))\right) \tag{20}$$

and

$$J_Z^B(x,z) = -\frac{n^B(x,z,t)}{m_B}\left(\gamma_{ZX}^{-1}(x,z)(\nabla_X\mu^B(x,z,t) + \nabla_X V^B(\mathbf{r})) + \gamma_{ZZ}^{-1}(x,z)(\nabla_Z\mu^B(x,z,t) + \nabla_Z V^B(\mathbf{r}))\right). \tag{21}$$

The inhomogeneous confinement keeps the tensorial structure of the friction of the tracer species due to its interaction with the majority species, A. The structure of the fluxes depends only on chemical potential gradients in the tracer species and in the direct effect of external fields on them. However, the friction coefficients depend functionally on the equilibrium, inhomogeneous, profiles of the majority species, $n^A(r)$, in the slit. In particular, the knowledge of $n^A(\mathbf{r})$ also allows, as shown in the following, to compute the non-uniform contact value of the pair correlation g^{AB} which is needed to evaluate the friction matrix. The structure of γ_{XZ} shows that only near a non-planar substrate, this matrix element is non-vanishing. In order to give an estimate of this quantity, we perform a Taylor expansion of the density and of the pair correlation in powers of the displacement $\sigma_{AB}\hat{\mathbf{s}}$ up to second order

$$\gamma_{XZ}(x,z) \approx \frac{8\sigma_{AB}^4}{15m^B}\sqrt{2\pi\mu_{AB}k_BT} \cdot \frac{\partial^2}{\partial x\partial z}[n^A(x,z)g_{AB}^{bulk}(\bar{\eta}(x,z))] \tag{22}$$

and observe that for the appearance of non-diagonal friction tensor elements, it is necessary to have non-vanishing cross derivatives $\frac{\partial^{m+n}n^A(x,z)g_{AB}^{bulk}(\bar{\eta}(x,z))}{\partial^m x\partial^n z} \neq 0$, with m,n odd integers. These terms vanish as we move away from the interfaces, where the n^A profile becomes nearly constant. Moreover, to zeroth order in the gradients of the density of the A particles, the off-diagonal matrix element vanishes because of the parity of the integrals.

The present treatment generalizes the method proposed by Davis and coworkers to nonflat confining surfaces and allows to treat also mixtures with finite concentrations of host particles. However, in this case, the friction matrix is time dependent since the motion of the B particles affects the configuration of the majority species (A particles). Moreover, also the interactions among the B particles would give a finite contribution to the friction matrix.[24]

The off-diagonal component of the friction matrix due to the inhomogeneous confinement affects the overall longitudinal diffusion of the tracers along the channel. From Eqs. (20) and (21), in the absence of a net transverse flux, $J_Z = 0$, the response to an applied force along the channel (or equivalently the relaxation of an equilibrium fluctuation) is characterized by the effective longitudinal diffusion coefficient,

$$D_{XX}(x,z) = \frac{k_BT}{m^B}\gamma_{XX}^{-1}(x,z) \tag{23}$$

which has the explicit form,

$$D_{XX}(x,z) = \frac{\gamma_{ZZ}(x,z)}{\gamma_{XX}(x,z)\gamma_{ZZ}(x,z) - \gamma_{XZ}(x,z)^2} = \frac{1}{\gamma_{XX}(x,z)}\left[1 - \frac{\gamma_{XZ}(x,z)^2}{\gamma_{XX}(x,z)\gamma_{ZZ}(x,z)}\right]^{-1}. \tag{24}$$

Eq. (24) shows that, due the positivity of the matrix γ_{ij}, the net effect of the off-diagonal terms is to enhance the diffusivity along the longitudinal direction. The magnitude of such an enhancement depends on that of the off-diagonal term in Eq. (16). In order to characterize the magnitude of such contributions, we use Eq. (22) into (24) getting

$$\frac{\gamma_{XZ}^2(x,y)}{\gamma_{XX}(x,y)\gamma_{ZZ}(x,y)} \simeq \left(\frac{\sigma_{AB}^2}{Lh}\frac{n^Am^A}{\rho}\right)^2. \tag{25}$$

The last expression shows that if the particle-particle distance at contact, σ_{AB}, is smaller than the channel width $2h$ and the channel varies smoothly, $h \ll L$ (so that $\frac{\gamma_{XZ}^2(x,y)}{\gamma_{XX}(x,y)\gamma_{ZZ}(x,y)} \ll 1$), we can expand Eq. (24) obtaining

$$D_{XX}(x,z) \simeq \frac{1}{\gamma_{XX}(x,z)}\left[1 + \frac{\gamma_{XZ}(x,z)^2}{\gamma_{XX}(x,z)\gamma_{ZZ}(x,z)}\right] \simeq \frac{1}{\gamma_{XX}(x,z)}\left[1 + \left(\frac{\sigma_{AB}^2}{Lh}\frac{n^Am^A}{\rho}\right)^2\right] \tag{26}$$

that captures the translational diffusivity enhancement along the longitudinal direction. The second relation in Eq. (26) provides an order of magnitude estimate of the impact that channel corrugation has on the enhancement of longitudinal diffusion. Hence, the time evolution of distribution of particles in an inhomogeneous environment will experience a faster broadening as compared to the case of the same distribution

in a homogeneous environment. It is interesting to note that such a result can be extended to other scenarios where the off-diagonal terms in γ_{ij} have a different physical origin, *e.g.,* when they are induced by spatial variations of an imposed potential.

V. EFFECTIVE ONE DIMENSIONAL DIFFUSION EQUATION *à la* FICK-JACOBS

The diffusion equation for the tracer species in the corrugated channel, Eq. (19), requires solving a two dimensional elliptic partial differential equation which can be numerically involved. In fact, even the determination of the steady current, $\mathbf{J}^B(x,z)$, generated by an externally imposed gradient of concentration or by a force field can become numerically intensive. When the corrugation of the walls is slowly varying, one can further approximate the diffusion process and obtain a mathematically simpler description following the arguments originally proposed by Jacobs.[13] Here, we shall use a method closely related to the one introduced by Zwanzig[14] which eliminates the transverse degrees of freedom assuming a fast equilibration of the density profile in the transverse direction, z.[36] The validity of the resulting effective one dimensional equation, referred to as Fick-Jacobs equation, has recently been confirmed,[17,37–40] who also considered the functional forms of higher order correction to the effective one dimensional dynamics.

If the channel width varies slowly, $\nabla_x h << 1$, one can assume that the tracer distribution equilibrates on a time scale faster than the one needed to reach equilibrium along the direction of the variation of the channel section. Accordingly, the transverse equilibrium condition for the B-particles reads

$$\nabla_Z(\mu^B(x,z) + V^B(x,z)) = 0 \tag{27}$$

and the continuity Eq. (19) can be reduced to

$$\frac{\partial n^B(x,z,t)}{\partial t} = \frac{1}{k_B T}\left[\nabla_X \gamma^{-1}_{XX}(x,z) + \nabla_Z \gamma^{-1}_{ZX}(x,z)\right] \cdot \left(n^B(x,z,t)\nabla_X \mu^B(x,z,t) + n^B(x,z,t)\nabla_X V^B(\mathbf{r})\right). \tag{28}$$

To use the information contained in (27), we separate the local chemical potential μ^B into its ideal gas contribution and the interacting part,

$$\mu^B(x,z,t) = k_B T \ln n^B(x,z,t) + \mu^B_{int}(x,z,t), \tag{29}$$

assuming that the tracer density can be decomposed in its concentration along the channel, $c(x,t)$, and the conditional density across the channel section, P,

$$n^B(x,z,t) = c(x,t)P(z|x) \tag{30}$$

and substitute this expression in Eq. (27). The conditional density profile, $P(z|x)$, is obtained from the equilibrium condition in the transverse direction, for any choice, of $c(x,t)$,

$$P(z|x) = \frac{e^{-\beta(\mu^B_{int}(x,z)+V^B(x,z))}}{\int_{-\infty}^{\infty} dz e^{-\beta(\mu^B_{int}(x,z)+V^B(x,z))}}. \tag{31}$$

Zwanzig showed that with this factorization, one can deduce the Fick-Jacobs equation for a two-dimensional potential for non-interacting diffusing particles.[14] Deviations from this conditional local equilibrium can be included still in an effective, generalized Fick-Jacobs equation where the diffusion coefficient depends on the channel shape.[14,21,40] For interacting systems, and following Zwanzig, one interprets $P(z|x)$ as the local equilibrium distribution of z conditional on a given x. For simplicity, we will always assume that the local equilibrium factorization, Eq. (30), holds. Accordingly, the results we will derive will generalize the original Fick-Jacobs equation for interacting systems. It is worth stressing that in the tracer limit, $\mu^B_{int}(x,z)$ only depends on n^A, but not on n^B so that it is a quenched variable.

The factorization assumption, Eq. (30), allows us to arrive at a simplified expression for the diffusive fluxes of tracer particles, whose component along the channel reads

$$J^B_X(x,z) = -\frac{c(x,t)}{k_B T}P(z|x)\gamma^{-1}_{XX}(x,z)\Big(\frac{k_B T}{c(x,t)}\nabla_X c(x,t) + \frac{k_B T}{P(z|x)}\nabla_X P(z|x) + \nabla_X \mu^B_{int}(x,z) + \nabla_X V^B(x,z)\Big) \tag{32}$$

while its normal component can be expressed as

$$J^B_Z(x,z) = -\frac{c(x,t)}{k_B T}P(z|x)\gamma^{-1}_{ZX}(x,z)\Big(\frac{k_B T}{c(x,t)}\nabla_X c(x,t) + \frac{k_B T}{P(z|x)}\nabla_X P(z|x) + \nabla_X \mu^B_{int}(x,z) + \nabla_X V^B(x,z)\Big). \tag{33}$$

The homogenization approximation implies that both flux components depend only on the concentration gradients along the channel. The inhomogeneous nature of the channel is encoded in the effective friction matrices and the expressions for the density profits and excess chemical potentials.

The net particle flow along the channel, I_x, can be obtained averaging the longitudinal component over the local channel

section for no-flux boundary conditions across the channel walls (see Appendix A),

$$I_X(x) = \int dz J_X^B(x,z) = -\mathcal{D}_{XX}(x)\left(\nabla_X c(x,t) + c(x,t)\beta\nabla_X \mathcal{A}(x)\right), \quad (34)$$

where

$$\beta\mathcal{A}(x) = -\ln\left(\frac{1}{L}\int_{-\infty}^{\infty} dz e^{-\beta(\mu_{int}^B(x,z)+V^B(x,z))}\right) \quad (35)$$

is the effective potential accounting for both the confinement and the interactions with the A particles encoded in μ_{int}. Interestingly, $\mathcal{A}$ can be regarded as a free energy, being the logarithm of the integral of the Boltzmann factor. Although we have introduced the prefactor $\frac{1}{L}$ in Eq. (35) for dimensional reasons, its magnitude is irrelevant in the subsequent analysis since only derivatives of $\mathcal{A}$ affect particle dynamics. In Eq. (34), we have introduced the pore averaged diffusion, $\mathcal{D}_{XX}$, one component of the pore averaged diffusion matrix

$$\mathcal{D}_{ij}(x) = \int_{-\infty}^{\infty} dz P(z|x)|D_{ij}(x,z)|, \quad (36)$$

which is very similar to the pore averaged diffusivity proposed by Davis and coworkers.[33] Eq. (34) generalizes the Fick-Jacobs equation to systems of interacting particles in the tracer limit and, for non-interacting particles, $\mu_{int} \to 0$, takes the form of the standard entropic potential contribution to particle transport along a corrugated channel, where the diffusion matrix is diagonal and with components that become constant. It is worth pointing out that non-ideality leads to an effective position-dependent local diffusion coefficient from the homogenization process assuming that the density profiles can be factorized assuming local equilibrium, Eq. (30). For ideal systems, a position-dependent diffusion coefficient arises from deviations in the density profile from Eq. (30). These changes have been obtained performing higher-order perturbation theories from the original Fick-Jacobs equation.[14,21,40] This difference shows that the origin of the inhomogeneous effective diffusion after homogenization for interacting systems is qualitatively different from the effective, local diffusion derived for ideal systems in the framework of the Fick-Jacobs equation. A generalization of the density profile beyond Eq. (30) for non-ideal systems, outside the scope of this paper, will clarify the relative relevance of the different contributions to a local, position-dependent, diffusion matrix for highly corrugated channels.

Eq. (32) shows that the flux along the channel is only a function of the local D_{XX} component of the pore averaged diffusion matrix. However, the transverse flux, Eq. (33), will depend on the cross component D_{XZ}, which does not vanish only for interacting systems in corrugated channels.

Although the procedure described can be easily extended beyond the tracer limit, the results obtained are formal and more complex to use because the friction matrix depends in general on the concentration of both A and B particles, which depend now on time. Notice that $V^B(x,z)$ and $\mu_{int}^B(x,z)$ are known because in the tracer limit they depend only on the majority species A, so that $P(x|z)$ is time independent. Current intensity (34) contains a one dimensional diffusive term, a drift term due to the interactions with the B particles and the walls, and an entropic term due to the non-uniform shape of the channel.

Since at steady state I_X must be constant on every section, due to particle number conservation, we can express the evolution equation for the tracer density,$c(x)$, simply as

$$\frac{dc(x)}{dx} + \beta\frac{d\mathcal{A}(x)}{dx}c(x) = -\frac{I_X}{\mathcal{D}_{XX}(x)}, \quad (37)$$

which can be expressed as a quadrature

$$c(x) = e^{-\beta\mathcal{A}(x)}\left[-I_X\int_0^x \frac{e^{\beta\mathcal{A}(s)}}{\mathcal{D}_{XX}(s)}ds + e^{\beta\mathcal{A}(0)}c(0)\right]. \quad (38)$$

At equilibrium, since $I_X = 0$, the tracer species steady state density profile reduces to its equilibrium shape

$$c(x) = e^{-\beta\mathcal{A}(x)}e^{\beta\mathcal{A}(0)}c(0), \quad (39)$$

as expected.

VI. RESULTS

After having obtained the relevant effective transport equations and density profiles for the tracers along a generic channel, in this section, we will analyze in more detail the effects that the inhomogeneities in the distribution of A particles and/or the channel corrugation have on the transport properties of the system. The slit is defined by the condition that the centers of the A particles have their transverse coordinate $-h(x) < z < h(x)$ and for $h(x)$, we assumed the functional form

$$h(x) = h_0 + \Delta\cos\frac{2\pi}{L}x.$$

The density profile $n^A(z,x)$ can be obtained independently and numerically by discretizing Eq. (18) on a two dimensional grid in the (x,z) domain. The solution is determined by an iterative process which was terminated when the difference between the profiles relative to the n-th and (n − 1)-th iteration was less than a relative tolerance 10^{-10}. Using the $n^A(z,x)$ profile as an input, we can compute the inhomogeneous pair correlation function and the matrix elements of the friction tensor.

We consider first a channel with planar walls as a reference geometry where the geometrical constraint does not lead to an x-dependent modulation in the transport coefficient, yet the presence of a boundary affects the local density of A-particles, as shown in Fig. 1(b). In particular, in the vicinity of the walls, the profiles vary rapidly over molecular length scales due to the action of the confining walls. The inhomogeneous density leads to a dependence in the friction matrix. As shown in Fig. 1(a), both elements of the friction matrix decrease upon approaching walls, whereas near the center of the slit, they both approach their bulk isotropic value given by Eq. (10). By inverting the friction matrix, via Eq. (23), we can compute the diffusion matrix elements. As shown in Fig. 1(b), the non-homogeneous density profiles lead to an increase of the local diffusion coefficients. In particular, the transverse diffusion coefficient D_{ZZ} results to be larger than the longitudinal diffusion coefficient, D_{XX} as shown in Fig. 1 due to the reduced rate of collision along the normal direction caused by the presence of the wall (see Appendix B). D_{XX} characterizes the

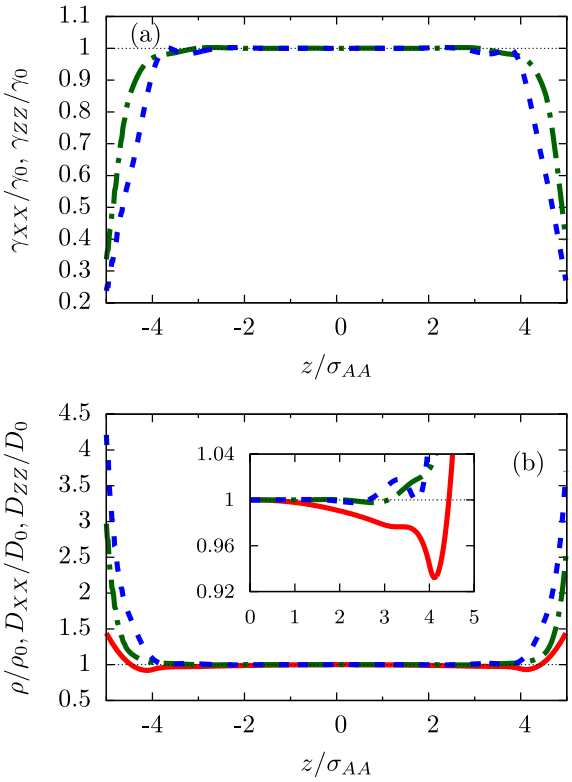

FIG. 1. Flat walls. (a) Friction matrix elements γ_{XX} (green dotted-dashed line) and γ_{ZZ} (blue dashed line) as a function of the distance from the center of the pore normalized by the particle size σ_{AA}. (b) Density profiles (red solid line), normalized by its values at the center of the channel, $\rho_0 = 0.2$, and D_{XX}, D_{ZZ} (green dotted-dashed and blue dashed lines, respectively) normalized by their values at the center of the channel as a function of the transverse coordinate, z, normalized by the channel half-section, h_0. Inset: zoom of the main panel.

diffusion of tracer articles along the channel. For impermeable walls, the diffusion transverse to the channel, and proportional to D_{ZZ}, is essentially a transient process. Finally, we may expect that in the presence of wetting layers adjacent to the walls, the friction tensor may increase due to the presence of a region of higher density close to the wall leading to a reduction of the local diffusion coefficient.

We quantify the channel corrugation through the parameter

$$\Delta S = \ln\left[\frac{h_{max}}{h_{min}}\right]. \tag{40}$$

The dependence of the density profile of A particles upon channel amplitude is captured in Fig. 2(a). As shown in the inset of Fig. 2(a), for a slowly varying channel, the density profiles essentially collapse in a unique curve if the density is plotted as a function of their distance to the wall. Therefore, the variation of channel amplitude modulates the overall density profile but not at length scales comparable to the size of A particles.

As sown in Fig. 2, for corrugated walls, the variations in the local channel amplitude lead on one hand to a modulation of both D_{XX} and D_{ZZ} (see Figs. 2(b) and 2(d), respectively), and on the other hand to a non-vanishing contribution to the off-diagonal term D_{XZ} (see Fig. 2(c)). In contrast to the density profiles, which collapse on a master curve in the vicinity of the channel wall, even though the modulations of D_{XX} and D_{ZZ} approach a master curve when plotted as a function of the rescaled distance from the wall δz, as shown in the insets of Figs. 2(b) and 2(d), they show larger deviations from a master curve when compared to Fig. 2(a). Analogous to the flat channel, we always find the transverse diffusion larger than the longitudinal one, $D_{ZZ} > D_{XX}$, whereas for corrugated channels, the off-diagonal contribution, D_{XZ}, does not vanish and, as expected, has a magnitude smaller than observed for the diagonal terms of the diffusion matrix. Moreover, it is interesting to note that while D_{XX} and D_{ZZ} are symmetric about the channel longitudinal axis, D_{XZ} is antisymmetric. Therefore, particles above (below) the channel longitudinal axis will experience a local "drift" towards the closest channel wall that reflects in a positive (negative) off-diagonal mobility $\mu = \beta D_{XZ}$ that can lead to an excess accumulation of particles on channel walls when B particles are driven by an external force.

Fig. 3 shows that the dependence of the average diffusion coefficients, $\mathcal{D}_{XX}$, $\mathcal{D}_{ZZ}$, and $\mathcal{D}_{XZ}$, is enhanced by increasing ΔS. Interestingly, both $\mathcal{D}_{XX}$ and $\mathcal{D}_{ZZ}$ attain their maximum value in the channel bottleneck, $x = 0$. In particular, while $\mathcal{D}_{XX}$, Fig. 3(a), shows a broader dependence on the longitudinal coordinate, $\mathcal{D}_{ZZ}$, Fig. 3(c) is more sensitive around the channel bottleneck, $x = 0$. In contrast, Fig. 3(b) shows that the maximum of $\mathcal{D}_{XZ}$ is not obtained in the channel bottleneck and that its position is ΔS-dependent. Showing the variation of the maximum value of the different components of the diffusion matrix as a function of the channel corrugation highlights the impact that geometrical variations have on the diffusion of trace particles, see Fig. 3(d). For the diagonal components, one can see increases of tens of a percent for the longitudinal component of the diffusion and up to 50% for the transverse one. This plot also highlights that the off-diagonal component becomes non-zero exclusively as a result of the corrugation in an interacting system and that the increase in its value is linear in ΔS.

Both the inhomogeneities in the density of the solvent species (A-particles) across the channel and the channel corrugation affect the net transport properties of the system. In particular, our framework allows us to analyze systematically the impact that the channel corrugation has on the mean particle flows. To this end, we analyze the particle flux induced by an applied, uniform external field when the channel is in contact with two reservoirs kept with equal chemical potentials. For what concerns the dependence of the net flux on the channel geometry, imposing periodic boundary conditions, $c(-L/2) = c(L/2)$ in Eq. (37) and assuming the symmetry of the channel, $h(x) = h(-x)$, we obtain expressions for the flux under the action of a constant driving force, F_0, in the flat channel and in the corrugated channel cases, I_f and I_c, respectively,

$$I_{f,c} = c_{f,c}(L/2)e^{\beta(\mathcal{A}_{f,c}(L/2)-fL/2)}(e^{\beta F_0 L}-1) \cdot \left[\int_{-L/2}^{L/2}\frac{e^{\beta(\mathcal{A}_{f,c}(x)-F_0 x)}}{\mathcal{D}_{XX,f,c}(x)}dx\right]^{-1}, \tag{41}$$

where $\Delta\mathcal{A}_{f,c} = \mathcal{A}_{f,c}(L) - \mathcal{A}_{f,c}(0)$ and $\mathcal{A}_{f,c}$ stands for the equilibrium free energy for a flat or a corrugated channel, as defined in Eq. (35), and $\mathcal{D}_{XX,f,c}(x)$ equals $\mathcal{D}_{XX}$ calculated, respectively, for a flat or corrugated channel.

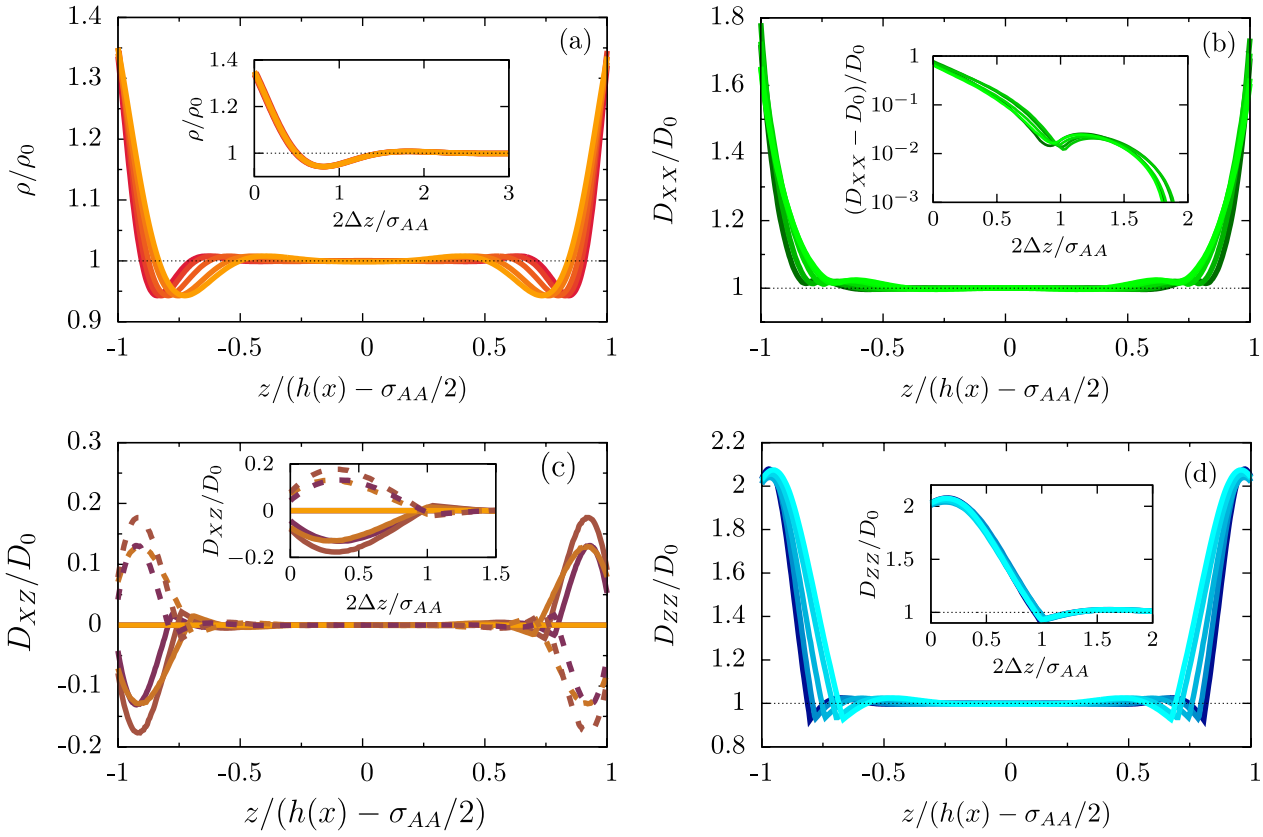

FIG. 2. Corrugate walls ($\Delta S = 0.2$ for all panels). (a) Density profile, normalized by the bulk value $\rho_0 = 0.2$, of A particles as a function of the transverse distance, normalized by the local channel half-amplitude $h(x)$, for different longitudinal positions, $x = 0, L/8, L/4, 3L/8, L/2$ standing lighter colors for larger values of x. (b), (c), and (d) Components of the diffusion tensor profile XX (panel b), XZ (panel c), and ZZ (panel d) component, normalized by the bulk value D_0, as a function of the transverse distance, normalized by the local channel half-amplitude $h(x)$, for different longitudinal positions, $x = 0, L/8, L/4, 3L/8, L/2$ (solid lines) and $x = -L/8, -L/4, -3L/8$ (dashed lines) standing lighter colors for larger values of $|x|$. (Note that in panels (b) and (d), the dashed lines coincide with the solid one for symmetry reasons.) Insets: dependence of the respective diffusion tensor profile as a function of the absolute distance from the channel wall, $\Delta z = h(x) - |z|$, normalized by the A particle diameter, σ_{AA}.

The ratio of the mean fluxes in the corrugated and flat channels, I_c/I_f, gives

$$\frac{I_c}{I_f} = \frac{c_c(L/2)e^{-\beta\mathcal{A}_c(L/2)}}{c_f(L/2)} e^{-\beta F_0 L/2} \frac{e^{\beta F_0 L} - 1}{\beta \mathcal{D}_{XX,f}(L/2) f} \cdot \left[\int_{-L/2}^{L/2} \frac{e^{\beta(\mathcal{A}_c(x) - fx)}}{\mathcal{D}_{XX,c}(x)} dx\right]^{-1}, \tag{42}$$

where we have exploited the fact that for a flat channel $\int_{-L/2}^{L/2} \frac{e^{\beta(\mathcal{A}_f(x) - F_0 x)}}{\mathcal{D}_{XX,f}(x)} dx = \frac{e^{\beta\mathcal{A}_f(L/2)}}{\mathcal{D}_{XX,f}(L/2)}(e^{\beta F_0 L} - 1)$. For a weakly corrugated channel, $\beta\mathcal{A} \ll 1$ we can expand the diffusion coefficients with respect to the reference, flat channel, $\mathcal{D}_{XX,c}(x) = \bar{\mathcal{D}}_{XX,c} + \tilde{\mathcal{D}}_{XX,c}(x)$. Accordingly, we can expand the last integral in Eq. (42) for small $\beta(\mathcal{A}_f(L/2) - F_0 L)$ and $\tilde{\mathcal{D}}_{XX,c}(x)$ up to second order getting

$$\int_{-L/2}^{L/2} \frac{e^{\beta(\mathcal{A}_c(x) - F_0 x)}}{\mathcal{D}_{XX,c}(x)} dx \simeq \frac{1}{\bar{\mathcal{D}}_c} \int_{-L/2}^{L/2} 1 + \beta(\mathcal{A}_c(x) - F_0 x) - \frac{\tilde{\mathcal{D}}_{XX,c}(x)}{\bar{\mathcal{D}}_{XX,c}} + \frac{1}{2}\beta^2(\mathcal{A}_c(x) - F_0 x)^2 + 2\frac{\tilde{\mathcal{D}}^2_{XX,c}(x)}{\bar{\mathcal{D}}^2_{XX,c}} - \beta\mathcal{A}_c(x)\frac{\tilde{\mathcal{D}}_{XX,c}(x)}{\bar{\mathcal{D}}_{XX,c}} dx, \tag{43}$$

where we have assumed $\tilde{\mathcal{D}}_{XX,c}(x) \ll \bar{\mathcal{D}}_{XX,c}$. Without loss of generality, we can assume $\int_{-L/2}^{L/2} \tilde{\mathcal{D}}_{XX,c}(x) dx = 0$. Accordingly, the last expression reduces to

$$\int_{-L/2}^{L/2} \frac{e^{\beta(\mathcal{A}_c(x) - F_0 x)}}{\mathcal{D}_{XX,c}(x)} dx \simeq \frac{1}{\bar{\mathcal{D}}_{XX,c}} \left[L + \beta(\tilde{\mathcal{A}}_c - F_0 L) + \int_{-L/2}^{L/2} \frac{1}{2}\beta^2 \mathcal{A}_c^2(x) + 2\frac{\tilde{\mathcal{D}}^2_{XX,c}(x)}{\bar{\mathcal{D}}^2_{XX,c}} - \beta\mathcal{A}_c(x)\frac{\tilde{\mathcal{D}}_{XX,c}(x)}{\bar{\mathcal{D}}_{XX,c}} dx\right] \tag{44}$$

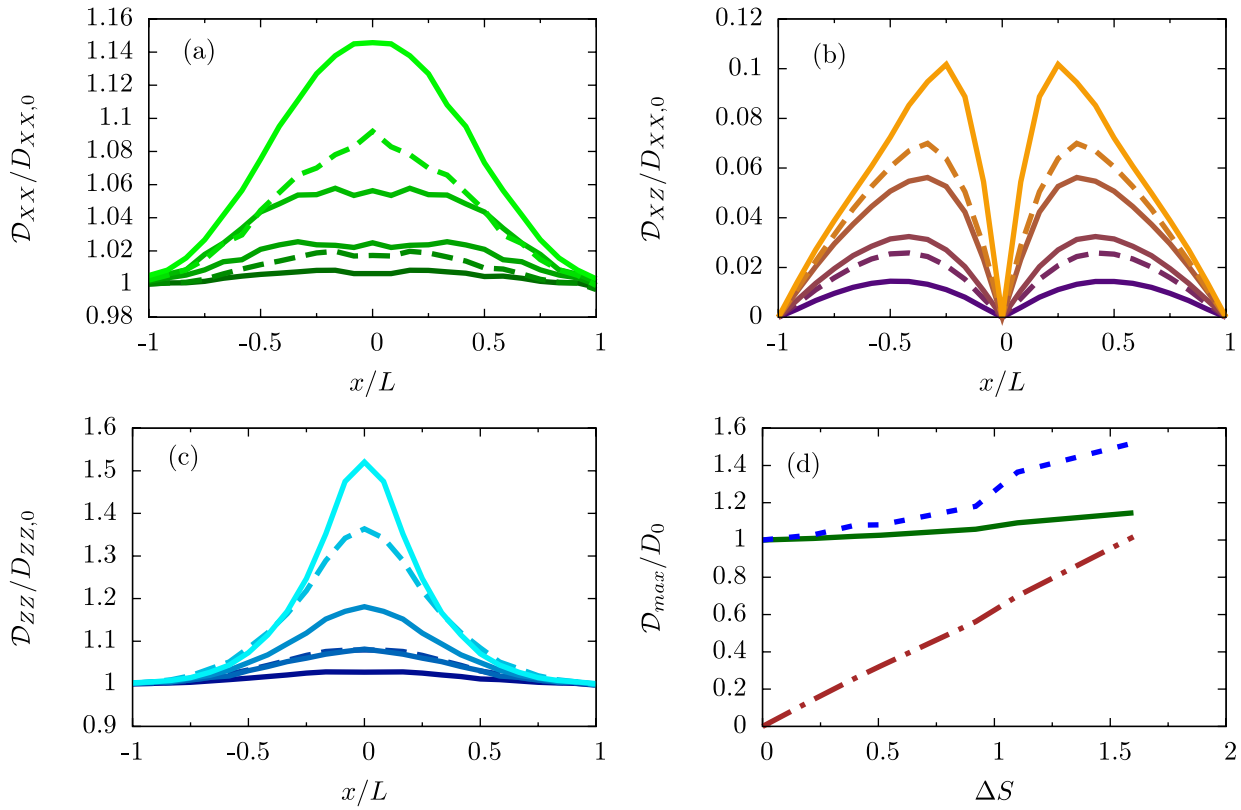

FIG. 3. Dependence of $\mathcal{D}_{XX}$ (a), $\mathcal{D}_{XZ}$ (b), and $\mathcal{D}_{ZZ}$ (c) as a function of the longitudinal position for different values of the entropic barrier $\Delta S = 0.22, 0.4, 0.51, 0.92, 1.1, 1.6$ standing lighter colors for larger values of ΔS (solid lines are for channels whose maximum amplitude is $10\sigma_{AA}$ while dashed lines for channel whose maximum amplitude is $6\sigma_{AA}$). (d) Dependence of the normalized maximum value of $\mathcal{D}_{XX}$ (solid line), $\mathcal{D}_{ZZ}$ (dotted line), and $\mathcal{D}_{XZ}$ (dashed-dotted line, magnified by a factor of 10 for clarity shake) as a function of ΔS.

which indicates, interestingly, that the tracer flux in a corrugated channel is reduced by an amount controlled by the modulation amplitude in both $\mathcal{A}$ and $\mathcal{D}$. Moreover, the presence of the cross term $-\int_{-L/2}^{L/2} \beta \mathcal{A}_c(x) \frac{\tilde{\mathcal{D}}_{XX,c}(x)}{\tilde{\mathcal{D}}_{XX,c}} dx$ reduces the overall flux. In principle, this contribution can lead to flux reversal and, in any case, indicate that there will exist an optimal channel shape that maximizes the net flux of tracer particle along the channel.

VII. CONCLUSIONS

We have analyzed the impact that channel corrugation has on diffusive particle transport. To this end, we have developed a framework that allows us to capture the coupling between the intrinsic inhomogeneities due to the microscopic properties of the medium and the modulations in the channel amplitude. In particular, we have focused on the equilibrium as well as transport properties of a very dilute suspension (tracer limit) of particles, B, moving through an environment formed by larger particles, A, when the overall system is confined between two corrugated plates. The interplay between spatial corrugation and non-ideality leads to a new type of inhomogeneity in the effective diffusion of tracer particles along a channel, absent for ideal diffusing particles. The diffusion process is characterized by a matrix where all its components depend on the local position along the channel. Channel corrugation also leads to the development of a new, off-diagonal term in the mobility matrix for non-ideal systems.

As a reference, we have characterized the density profile as well as the diffusion coefficients of the solute species (B-particles) in a flat channel, $\Delta S = 0$. Fig. 1(b) shows that the presence of the walls induces heterogeneities in the solvent density (A-particles) that ultimately affect the density and the diffusivities of B-particles. In particular, both the longitudinal, D_{XX}, and transverse, D_{ZZ}, diffusion coefficients increase upon approaching the wall. Such a behavior is due to the lack of A particles in the vicinity of the wall that eventually decreases the effective drag experienced by the B particle (see Appendix B).

For corrugated channels, we characterize their inhomogeneity in terms of a tuning parameter that measures the difference between maximal and minimal channel apertures, and that can be seen, effectively, as a measure of the geometric, or entropic resistance to particle flow, ΔS. For corrugated channels, when $\Delta S \neq 0$, the channel amplitude modulation leads to density profiles that depend on the channel local amplitude. Interestingly, the variation of channel amplitude only mildly affects the density profile of A particles. Accordingly, the density profiles for different amplitudes collapse on a master curve in a region close to channel walls. These modulations in particle A density eventually determine the effective diffusion coefficients of B particles. In particular, when $\Delta S \neq 0$, the off-diagonal terms D_{XZ} become non-vanishing therefore leading to a coupling between the longitudinal and transverse transport properties inside the channel. This new transport mechanism may be

relevant since it indicates a new transport mechanism that will affect the effective permeability across inhomogeneous membranes.

Fig. 2(c) shows the most striking effect of the mesoscopic modulation of channel amplitude, namely, the appearance of off-diagonal terms, D_{XZ} in the diffusion matrix of B particles. This new term appears due to a coupling between the change in the channel cross section and the interaction between particles. It is not present for non-ideal systems when the density profiles satisfy local equilibrium. Interestingly D_{XZ} is antisymmetric with respect to the transverse coordinate. Therefore, for systems under an external weak force (for which the linear response holds), we expect an excess of accumulation of B particles towards the channel walls in the first half of the channel and the opposite in the second half, compare solid and dashed lines in Fig. 2(c).

Since the modulation of the diffusion coefficients depends on the position of the particles along the channel, the overall relevance of the modulation of channel amplitude on the diffusion coefficient is better captured by the average quantities, $\mathcal{D}_{XX}$, $\mathcal{D}_{XZ}$, and $\mathcal{D}_{ZZ}$. Fig. 3 shows that all the components of the diffusion matrix grow upon increase of ΔS. In particular, Fig. 3(d) shows that $\mathcal{D}_{XZ}$ is the most sensitive component to changes in the channel corrugation and that it depends linearly on ΔS. From the point of view of the impact that channel modulation has on the absolute magnitude of the diffusion coefficients for the solute, Fig. 3(d) shows that for the system under study, namely, hard sphere suspension, those modulations are of the order of some tens of a percent and, in order to increase them further more corrugated channels are needed therefore limiting the possible relevance of the phenomena describe here. In particular, here we focused on the case of hard sphere suspensions (for which an analytical form for the two point correlation function is provided) that introduce a typical length scale, namely, the sphere radius $\sigma_{AA}/2$. Therefore, for hard spheres suspension, the bottleneck of the channel cannot be smaller than σ_{AA} and, namely, cannot be smaller than the characteristic length. However, recently it has been shown that when the typical length characterizing the microscopic interactions is comparable to the channel bottleneck, the coupling between the microscopic properties of the medium and the mesoscopic properties of the channel is maximized.[11] Therefore, we expect an amplification of the phenomena we have described for hard sphere suspension in systems characterized by a typical interaction length that is larger than the hard-core repulsion such as fluids, polymer suspensions, or in electrolytes[11] just to mention a few among others that allows for a better overlap between the microscopic interaction length and the channel bottleneck.

ACKNOWLEDGMENTS

U.M.B.M. acknowledges the support received from the European Science Foundation (ESF) for the activity entitled "Exploring the Physics of Small Devices (EPSD)" under the Grant No. 3720. I.P. acknowledges the Dirección General de Investigación (Spain) and DURSI for financial support under Project Nos. FIS 2011-22603 and 2014SGR-922, respectively, and *Generalitat de Catalunya* under program *Icrea Academia*. I.P. declares that the research leading to these results has received funding from the European Union Seventh Framework Programme (No. FP7-PEOPLE-2011-IIF) under Grant agreement No. 301214 (http://ec.europa.eu/research/fp7/index_en.cfm).

APPENDIX A: BOUNDARY CONDITIONS

Here, we show that since in the stationary state, the B-current is solenoidal,

$$\nabla \cdot \mathbf{J}^B(x,z) = 0 \tag{A1}$$

and the current intensity, I_X, along the axial direction must be uniform in space. Integrating Eq. (A1) over z, we obtain in the hard walls case the relation,

$$\int_{-h(x)}^{h(x)} dz \nabla_X J_X^B(x,z) + J_Z^B(x,h(x)) - J_Z^B(x,-h(x)) = 0, \tag{A2}$$

where the two boundary terms J_Z^B vanish only in the case of flat walls whose normals are parallel to the z direction (condition of impenetrability of the walls). In order to obtain a result for nonflat walls, we transform the first term of (A2) as

$$\int_{-h(x)}^{h(x)} dz \nabla_X J_X^B(x,z) = \nabla_X \int_{-h(x)}^{h(x)} dz J_X^B(x,z) - (J_X^B(x,h(x)) + J_X^B(x,-h(x)))\nabla_X h(x) \tag{A3}$$

and use the vanishing of the normal flux at the walls,

$$\mathbf{J}^B(x,\pm h(x)) \cdot \hat{\mathbf{n}}(x,\pm h(x)) = 0, \tag{A4}$$

where $\hat{\mathbf{n}}$ is the normal to the wall and explicitly we have

$$J_X^B(x,\pm h)\nabla_X h(x) \mp J_Z^B(x,\pm h) = 0. \tag{A5}$$

We substitute such a result in Eq. (A3) and using Eq. (A2), we finally obtain that the integral over z of the x component of the current $\mathbf{J^B}$ is independent of x,

$$\int_{-h(x)}^{h(x)} dz \nabla_X J_X^B(x,z) + J_Z^B(x,h(x)) - J_Z^B(x,-h(x)) = \nabla_X \int_{-h(x)}^{h(x)} dz J_X^B(x,z) = 0 \tag{A6}$$

that is J_x^B is constant on every section

$$\int_{-h(x)}^{h(x)} dz J_X^B(x,z) = I_X. \tag{A7}$$

APPENDIX B: SIMPLE ARGUMENT FOR UNDERSTANDING THE DECREASE OF THE FRICTION MATRIX ELEMENTS NEAR A HARD WALL

Here, we give a simple argument in order to justify the decrease of the friction matrix elements near a planar wall. The argument is based on a rough estimate of the collision time for normal and tangential motions of the tagged molecules. The scattering cross section for hard spheres of diameter σ under bulk conditions is $S = \pi\sigma^2$. If the particle moves at an average velocity $v_{th} = \sqrt{k_B T/m}$ through an assembly of hard spheres of density n^A, it will suffer the following number of collisions per unit time:

$$\mathcal{N}_{coll} = n^A S v_{th} = \frac{1}{\tau}, \tag{B1}$$

where τ is the average collision time which can be related to the friction coefficient by

$$\gamma = \frac{1}{\tau} = n^A \pi\sigma^2 v_{th}. \tag{B2}$$

Let us remark that $\pi\sigma^2 v_{th}$ is the volume of the cylinder of influence of the particle per unit time and that such a volume is reduced when the particle is at a distance from the wall less than σ.

It is reasonable to assume that in the proximity of a wall, both the normal friction and the tangential friction decrease because the tagged particle will encounter no particles in the region where the collision cylinder "intrudes" the wall. Regarding the normal friction such an effect could be modeled by replacing (B2) by

$$\gamma_{Normal}(z) = \pi\sigma^2 v_{th} \frac{\int_{z-\sigma}^{z+\sigma} dz' n^A(z')}{2\sigma}. \tag{B3}$$

The rationale of such a formula is the replacement of local density $n^A(z)$ by a coarse grained density obtained averaging it over a region of thickness σ, which is the region of influence of the hard sphere. Modeling the presence of the surface at $z = 0$ by a stepwise profile ($n^A(z) = 0$ for $z < \sigma/2$ and n_0^A otherwise), we have

$$\gamma_{Normal}(z) = n_b \pi\sigma^2 v_{th} \frac{\int_{z-\sigma}^{z+\sigma} dz' \theta(z' - \sigma/2)}{2\sigma} = n_0^A \pi\sigma^2 v_{th} \frac{\int_{max(z-\sigma,\sigma/2)}^{z+\sigma} dz'}{2\sigma} \tag{B4}$$

for $z < \sigma$

$$\gamma_{Normal}(z) = n_0^A \pi\sigma^2 v_{th} \frac{z + \sigma/2}{2\sigma} \tag{B5}$$

and for $z > \sigma$,

$$\gamma_{Normal}(z) = n_0^A \pi\sigma^2 v_{th}. \tag{B6}$$

In the case of the tangential motion of the B-molecule, the cylinder of influence will be smaller if the distance z between the particle and the wall is less than σ because part of the volume of the cylinder whose axis is parallel to the x-direction is not available to the target particles. We know that the area $A(z)$ of the circular segment (the overlap between a circle and a half-plane) as a function of the distance of the particle z from the wall if $\sigma/2 < z < \sigma$ is given by

$$A(z) = \frac{1}{2}\sigma^2(\theta - \sin\theta), \tag{B7}$$

where

$$\theta = 2\arccos(z/\sigma). \tag{B8}$$

Substituting

$$A(z) = \sigma^2\Big(\arccos(z/\sigma) - \frac{z}{\sigma}\sqrt{1 - (\frac{z}{\sigma})^2}\Big). \tag{B9}$$

Thus, the volume per unit time available to particle B to collide is reduced

$$V_{cyl} = \Big(\pi\sigma^2 - A(z)\Big) v_{th} \tag{B10}$$

and we find

$$\gamma_{Tangential}(z) = n_0^A V_{cyl} = n_b\Big(\pi\sigma^2 - A(z)\Big) v_{th}. \tag{B11}$$

[1] L. Bocquet and E. Charlaix, Chem. Soc. Rev. **39**, 1073 (2010).
[2] R. B. Schoch, J. Han, and P. Renaud, Rev. Mod. Phys. **80**, 839 (2008).
[3] R. M. Barrer, *Zeolites and Clay Minerals as Sorbents and Molecular Sieves* (Academic, New York, 1978).
[4] C. Calero, J. Faraudo, and M. Aguilella-Arzo, Phys. Rev. E **83**, 021908 (2011).
[5] L. Dagdug, A. M. Berezhkovskii, Y. A. Makhnovskii, V. Y. Zitsereman, and S. Bezrukov, J. Chem. Phys. **134**, 101102 (2011).
[6] E. Altintas, E. Sarajlic, F. K. Bohringerb, and H. Fujita, Sens. Actuators, A **154**, 123 (2009).
[7] D. Reguera, A. Luque, P. S. Burada, G. Schmid, J. M. Rubi, and P. Hänggi, Phys. Rev. Lett. **108**, 020604 (2012).
[8] P. Malgaretti, I. Pagonabarraga, and J. M. Rubi, Phys. Rev. E **85**, 010105(R) (2012).
[9] P. Malgaretti, I. Pagonabarraga, and J. M. Rubi, J. Chem. Phys. **138**, 194906 (2013).
[10] R. Eichhorn, J. Regtmeier, and P. Reimann, Soft Matter **6**, 1858 (2010).
[11] P. Malgaretti, I. Pagonabarraga, and J. M. Rubi, Phys. Rev. Lett. **113**, 128301 (2014).
[12] U. Marini Bettolo Marconi and S. Melchionna, J. Chem. Phys. **134**, 064118 (2011).
[13] H. Jacobs, *Diffusion Processes* (Springer-Verlag, New York, 1967).
[14] R. Zwanzig, J. Phys. Chem. **96**, 3926 (1992).
[15] D. Reguera and J. M. Rubi, Phys. Rev. E **64**, 061106 (2001).
[16] P. Kalinay and J. K. Percus, Phys. Rev. E **74**, 049904 (2006).
[17] P. Kalinay and J. K. Percus, Phys. Rev. E **78**, 021103 (2008).
[18] P. Kalinay and J. K. Percus, Phys. Rev. E **82**, 031143 (2010).
[19] P. Kalinay, Phys. Rev. E **87**, 032143 (2013).
[20] A. Berezhkovskii, M. Pustovoit, and S. Bezrukov, J. Chem. Phys. **126**, 134706 (2007).
[21] A. Berezhkovskii and A. Szabo, J. Chem. Phys. **135**, 074108 (2011).
[22] G. Chacn-Acosta, I. Pineda, and L. Dagdug, J. Chem. Phys. **139**, 214115 (2013).
[23] L. Dagdug and I. Pineda, J. Chem. Phys. **137**, 024107 (2012).
[24] U. Marini Bettolo Marconi and S. Melchionna, J. Chem. Phys. **135**, 044104 (2011).
[25] H. Van Beijeren and M. H. Ernst, Physica **68**, 437 (1973).
[26] H. Van Beijeren and M. H. Ernst, Physica **70**, 225 (1973).
[27] U. Marini Bettolo Marconi and S. Melchionna, J. Chem. Phys. **131**, 014105 (2009).
[28] M. Wendland, Fluid Phase Equilib. **141**, 25 (1997).

[29]J. Fischer and M. Methfessel, Phys. Rev. A **22**, 2836 (1980).
[30]T. Boublík, J. Chem. Phys. **53**, 471 (1970).
[31]G. Mansoori, N. Carnahan, K. Starling, and T. Leland, Jr., J. Chem. Phys. **54**, 1523 (1971).
[32]T. Vanderlick and H. Davis, J. Chem. Phys. **87**, 1791 (1987).
[33]H. T. Davis, J. Chem. Phys. **86**, 1474 (1987).
[34]I. Bitsanis, J. Magda, M. Tirrell, and H. Davis, J. Chem. Phys. **87**, 1733 (1987).
[35]J. Magda, M. Tirrell, and H. Davis, J. Chem. Phys. **83**, 1888 (1985).
[36]U. M. B. Marconi, S. Melchionna, and I. Pagonabarraga, J. Chem. Phys. **138**, 244107 (2013).
[37]D. Reguera, G. Schmid, P. S. Burada, J. M. Rubí, P. Reimann, and P. Hänggi, Phys. Rev. Lett. **96**, 130603 (2006).
[38]P. S. Burada, G. Schmid, D. Reguera, J. M. Rubí, and P. Hänggi, Phys. Rev. E **75**, 051111 (2007).
[39]P. Kalinay and J. Percus, Phys. Rev. E **74**, 041203 (2006).
[40]S. Martens, G. Schmidt, L. Schimansky-Geier, and P. Hänggi, Phys. Rev. E **83**, 051135 (2011).